forests

MDPI

Article

Genome-Wide Identification and Analysis of the *DGAT* Gene Family in *Lindera glauca* and Expression Analysis during Fruit Development Stages

Xue Bai [1], Yongyi Yang [1], Lun Xie [1], Qingqing Li [1] and Biao Xiong [1,2,*]

[1] College of Tea Science, Guizhou University, Guiyang 550025, China
[2] Department of Botany, College of Science, University of British Columbia, Vancouver, BC V6T 1Z4, Canada
* Correspondence: bxiong@gzu.edu.cn

Abstract: Diacylglycerol acyltransferase (DGAT) is a vital and sole rate-limiting enzyme involved in triacylglycerol synthesis. Identifying *DGAT* genes in *Lindera glauca* is essential for studying lipid metabolism pathways and developing novel oil crops with enhanced value. In the study reported in this paper, 15 *LgDGAT* family genes were first obtained from the *L. glauca* genome via bioinformatics analysis. We comprehensively analyzed their chromosome distribution, gene structure, subcellular localization, promoter prediction, phylogenetic relationships, tissue-specific expression, and expression patterns during different stages of fruit development. Our findings revealed that LgDGATs can be classified into DGAT1, DGAT2, DGAT3, and WSD (wax ester synthase/acyl-CoA: diacylglycerol acyltransferase) subfamilies distributed across chromosome 3, 5, 6, 8 and 11. *LgDGATs*' promoter region showed abundant elements linked to the light response and plant hormone response. Forms of *LgDGAT1*, *LgDGAT2*, and *LgDGAT3* were primarily expressed in the early and late phases of fruit development, indicating their potential function in the growth and development of *L. glauca*, particularly in oil accumulation. Conversely, *LgWSDs* exhibited predominant expression in stems and leaves. This paper elucidates the gene structure and expression patterns of *LgDGATs*, providing a theoretical foundation for understanding the functionality of *DGAT* genes in *Lindera* species.

Keywords: *DGAT* gene family; transcriptome; characteristic identification; expression pattern

Citation: Bai, X.; Yang, Y.; Xie, L.; Li, Q.; Xiong, B. Genome-Wide Identification and Analysis of the *DGAT* Gene Family in *Lindera glauca* and Expression Analysis during Fruit Development Stages. *Forests* **2023**, *14*, 1633. https://doi.org/10.3390/f14081633

Academic Editor: John E. Carlson

Received: 13 June 2023
Revised: 8 August 2023
Accepted: 11 August 2023
Published: 13 August 2023

1. Introduction

Triacylglycerol (TAG) serves as plants' primary lipid storage form and is valuable for human consumption and biofuel production [1]. Among the various pathways involved in TAG biosynthesis in different plant organs and tissues, the Kennedy pathway is one of the most critical [2,3]. Diacylglycerol acyltransferase (DGAT) is the only rate-limiting enzyme involved in this pathway's ultimate conversion of diacylglycerol (DAG) to TAG, and as such, it is crucial in controlling the amount of TAG present [4].

DGAT enzymes are categorized into four types based on their cell location and structural variations: DGAT1, DGAT2, DGAT3 and WS/DGAT (wax ester synthase/acyl-CoA: diacylglycerol acyltransferase) [5,6]. As genetically engineered targets for enhancing the yield of plant storage lipids, *DGAT1s* are crucial for the cultivation of oilseed crops [7,8]. They have also been associated with plant growth [9,10]. *Arabidopsis* seedlings mutant for *DGAT1* exhibit abnormal growth, shrunk seeds, reduced lipids content, and delay seed maturation [11,12]. Overexpression of *Arabidopsis AtDGAT1* in tobacco significantly increases TAG content in transgenic tobacco seeds [13]. *DGAT2* selectively accumulates unsaturated fatty acids in TAG. Overexpression of *PfDGAT2* in *Perilla frutescens* [14] and *JcDGAT2* in *Jatropha curcas* [15] increases their unsaturated fatty acid content, respectively. Additionally, *DGAT2* is co-expressed with transcription factor ethylene response factors in tobacco to promote the flow of carbon sources toward fat and fatty acid biosynthesis [16]. *DGAT3* is a plant cytoplasmic soluble metalloenzyme [17]. The accumulation of unsaturated fatty

acids was dramatically increased when *camelina CaDGAT3-3* was expressed specifically in tobacco [18]. *WS/DAGT* is an enzyme that possesses dual functionality as both a TAG synthetase and a wax ester synthase (WS), with its WS activity surpassing that of TAG synthetase [6]. *Arabidopsis AtWSD1* exhibits high level of WS activity, while DGAT activity is approximately tenfold lower than its WS activity [19]. Moreover, *AtWSD1* is crucial in producing epidermal wax, which is essential for plant moisture retention and salinity tolerance [20].

Lindera glauca (Sieb. et Zucc.) Blume is a deciduous shrub or small fruit tree found in lowland woodland forest margins in China, Japan, and Korea [21–23], where it undergoes non-fusion (seed asexual reproduction) [24] and sexual reproduction [25,26]. *L. glauca* is a secondary forest species in low and middle altitude area, and considered as a significant ecological and economic tree species due to its abundant resources, high adaptability, and ecological advantages in China [27]. The fatty acids and aromatic oils found in *L. glauca* fruits, as well as the terpenoids, flavonoids, and alkaloids that they contain, are rich in traditional medicinal uses [28]. The primary fatty acids in *L. glauca* fruits and seeds are capric acid, oleic acid, palmitic acid, and linoleic acid [29]. Fruits and essential oils produced in China annually amounts to 120,000 metric tons and 1000 kiloliters, respectively [30,31]. *L. glauca* fruit or seed oil is frequently utilized in food oils, biodiesel, or daily-use chemical goods, including soaps, surfactants, and lubricants [32–34].

However, there were limited studies on the biosynthesis and accumulation of oil in *L. glauca*, hindering the discovery of related genes and the improvement in oil content. Therefore, we gathered fruits, 60, 90, and 150 days after flowering to examine the expression of the *DGAT* family of essential genes for oil synthesis. Additionally, to gain comprehensive insights into the physicochemical properties, chromosome localization, conserved motifs, gene structure, evolutionary relationship and *cis*-acting elements of *LgDGATs*, we performed bioinformatics analysis of all *LgDGATs* in the whole genome. The findings will serve as a basis for further investigation into oil biosynthesis and accumulation in *L. glauca* fruits and the breeding of new varieties of in *L. glauca* fruits with high oil.

2. Materials and Methods

2.1. Identification and Characterization of DGAT Gene Family in L. glauca

The potential *LgDGAT* family members were identified and retrieved from the *L. glauca* genome sequence by downloading the Hidden Markov Model profiles of *DGAT* genes (PF03982) from the Pfam database (http://pfam.xfam.org/) (accessed on 20 July 2022) [35] using HMMER 3.0 (http://hmmer.janelia.org/) (accessed on 20 July 2022) software (E-value $\leq 1 \times 10^{-5}$) [36]. The *L. glauca* genome was searched using the *Arabidopsis DGAT* genes as a probe using the Blastp tool, and the candidate sequence with an E-value 1×10^{-10} was chosen after eliminating duplicates. The candidate sequences lacking the specific *DGAT* family protein domains were excluded using the CD-search program [37] (https://www.ncbi.nlm.nih.gov/Structure/bwrpsb/bwrpsb.cgi) (accessed on 20 July 2022), leaving the *LgDGATs*.

Utilizing the ProtParam tool (https://web.expasy.org/Protparam/) (accessed on 13 April 2023), each LgDGAT protein's physicochemical characteristics were predicted [38]. In addition, the Cell-PLoc 2.0 (http://www.csbio.sjtu.edu.cn/bioinf/Cell--PLoc--2/) (accessed on 13 April 2023) and TMHMM Server v. 2.0 (https://services.healthtech.dtu.dk/services/TMHMM--2.0/) (accessed on 13 April 2023) online tools were employed, respectively, for the prediction of subcellular locations and transmembrane domains [39].

2.2. Phylogenetic Analysis of LgDGATs

The rice (http://rice.plantbiology.msu.edu/) (accessed on 4 August 2022) and maize (https://maizegdb.org/) (accessed on 4 August 2022) databases, which contain the DGAT protein sequences of *Oryza sativa* and *Zea mays*, respectively, were used to download the data used in this study. The UniProt website (https://www.uniprot.org/), which contains the sequences for *Glycine max* and *Brassica napus*, were used to download the

data (accessed on 4 August 2022). ClustalW (http://www.clustal.org/clustal2/) (accessed on 19 April 2023) was used to align the protein sequences from *L. glauca*, *A. thaliana*, *O. sativa*, *Z. mays*, *G. max*, and *B. napus* in order to examine the evolutionary relationship between *LgDGATs* and other species *DGATs*. The aligned sequences were subsequently used to create a phylogenetic tree based on the maximum likelihood technique using MEGA-X (https://www.megasoftware.net/dload_win_gui) (accessed on 19 April 2023) with the default parameters and a bootstrap value set to 1000. The online tool iTOL (https://itol.embl.de/) (accessed on 19 April 2023) was used to enrich and show the resulting phylogenetic tree [40].

2.3. Motifs and Gene Structure Analysis

Using the MEME website (https://meme--suite.org/meme/tools/meme) (accessed on 26 April 2023) and the motif number was set to 20 to predict the conserved motif of the LgDGAT protein [41]. Next, the motif and gene structure of the *LgDGATs* were visualized using TBtools v1.120 software, combining the conserved motif data file and the genome database GFF3 file [42].

2.4. Cis-Acting Elements Analysis for LgDGAT Gene Promoters

The PlantCARE online website (http://bioinformatics.psb.ugent.be/webtools/plantcare/html/) (accessed on 27 July 2022) [43] was used to predict *cis*-acting elements from the sequences of *LgDGATs* that were 2000 bp upstream of the start codon. TBtools was used to display the results.

2.5. Chromosomal Distribution, Gene Duplication and Synteny Analysis of LgDGATs

Using the annotation file for the genome of *L. glauca*, the MapChart program was used to visualize the chromosomal position of *LgDGATs* [44]. Gene duplication events of *DGATs* and the collinearity relationships between intraspecies and interspecies were analyzed using MCScanX-2019 software [45]. The results were visualized using Circos 0.69 [46] and TBtools v1.120 software.

2.6. Calculation of the Ka/Ks Values

The non-synonymous replacement rate (*K*a) and synonymous replacement rate (*K*s) were calculated using the Simple *K*a/*K*s Calculator in TBtools software. The *K*a/*K*s ratio was explored to investigate the selection pressure on genes in the evolutionary process. Using the formula T = *K*s/(2 × 3.02 × 10^{-9}) × 10^{-6} million years (Mya), the divergence time (T) was calculated [47].

2.7. Expression of the LgDGAT Genes During Fruit Development

Transcriptome sequencing (RNA–Seq) experiments were conducted in three stages during fruit development of *L. glauca*: 60 (early fruiting stage), 90 (rapid fruit growth), and 150 (fruit ripening) days after flowering (DAF). The fruit samples were collected from the nursery (31.8° N, 114.1° E) of Jigongshan National Nature Reserve (Henan, China). Three replicates of each sample were frozen in liquid nitrogen and kept at ultra-low temperatures at –80 °C after being collected in the field. RNAprep Pure Plant Kit (TIANGEN, Germany) was used to extract total RNA from the obtained samples. Separate cDNAs were generated for each of the nine replicate RNA samples using the KAPA Stranded mRNA-seq Kit. Firstly, mRNA enrichment of total RNA was performed using RNA cleanXP purified magnetic beads with oligo(dT) produced by Beckman Coulter (USA). The mRNA is then broken into fragments by heating, and the first strand of cDNA is synthesized with random primers based on this template. RNase H is added to create a gap, and the RNA will continue to extend in the gap to generate a second strand of cDNA. The double-stranded cDNA is then purified, end-repaired, and the 3′ end is tailed. Finally, the obtained library DNA was amplified and purified using PCR, and fragments of 250~500 bp size were selected via agarose gel electrophoresis for recovery. The nine separate libraries were then barcoded,

and the barcoded libraries were normalized to ensure equal representation in the library pool prior to sequencing on the Illumina NovaSeq 6000 platform. The ID of each library can be found at NCBI (accession number: PRJNA977679). The extraction of total RNA, cDNA library construction and sequencing were carried out by Biomarker Technologies Ltd (Beijing, China). The sequencing results were submitted to NCBI (accession number: PRJNA977679). We employed the TPM method for expression quantification. Based on the differential expression of the *DGATs* in transcriptome annotation data, one-way analysis of variance (ANOVA) was performed using the IBM SPSS Statistic 26 [48], and the results were represented in a histogram using Pheatmap (https://cran.r--project.org/web/packages/pheatmap/) (accessed on 17 May 2023) package in R–4.0.0 software (https://www.r--project.org/) (accessed on 17 May 2023).

2.8. Real-Time PCR Analysis of LgDGATs' Gene Expression

After the samples were ground into powder with liquid nitrogen, total RNA was extracted using RNAprep Pure Kit (DP441, TIANGEN, Beijing, China). The NanoPhotometer N50 (Implen, Munich, Gemany) was used to detect RNA purity and concentration. Then, total RNA reverse transcription was carried out using PrimeScript™ RT Master Mix (TaKaRa, Tokyo). The reaction procedure was as follows: 37 °C for 15 min and 85 °C for 5 s. After the reaction was terminated, the samples were quickly placed on ice and stored in a refrigerator at –20 °C. Specific primers of 9 *LgDGATs* and internal controls were designed at NCBI (Table 1) (https://www.ncbi.nlm.nih.gov/tools/primer-blast/index.cgi?LINK_LOC=BlastHome) (accessed on 23 July 2023). *RPL32e* (large subunit ribosomal protein L32e) and *UBC* (ubiquitin-conjugating enzyme) were used as internal controls. The primers were all synthesized by TSINGKE Biotechnology Co., Ltd. (Beijing, China). The gene expression of 9 *LgDGATs* was analyzed with qRT-PCR, which was performed using CFX96 real-time PCR system (Bio-RAD, Laboratories, Hercules, CA, USA). The reaction system (25 μL) contained TB Green® Premix Ex Taq™ II 12.5 μL, upstream primers 1 μL, downstream primers 1 μL, cDNA 2 μL, and sterile distilled water 8.5 μL. The preparation process was completed on ice. Reaction conditions were as follows: 95 °C for 30 s, followed by 39 cycles at 95 °C for 5 s and 60 °C for 30 s, with a melting curve analysis. The operation was repeated three times for each sample. The $2^{-\Delta\Delta CT}$ method was then used to calculate the levels of gene expression.

Table 1. Primers for qRT-PCR.

Gene ID	Forward Primer	Reverse Primer
LgDGAT1	CGACTCCTCCTCCAAGACCTG	ACCGACGGATTCCTCTGTTCTC
LgDGAT2.1	TCAGTGAGGTTATCTGTTGC	GACCATAGCAGAAAACAGGA
LgDGAT2.2	CACACCACTACTAAGGCAAA	ATATGAACAATCTCCCGAGC
LgDGAT2.3	GAGGTCATCCTCCAGAAAAG	AAGTTGAGATGAATGGTCCC
LgDGAT2.4	GTGTTTGGGATGCTGTTATG	ACGTGAAGTGTAATGGGAAA
LgDGAT2.6	CTCTGTCAACGCAACCATACTCAC	TGTGGACTGTGGTGTGGATGG
LgDGAT3.3	ATAGACCAACCACAACCCATTCAG	AAGAGAAGCAAGGAACAGCAGTAG
LgWSD1	TCCCAAGCCAGTCCAGTGTC	TTGAGATTGTGAAGGTTGTGTTAGC
LgWSD2	AAGTTTCGACATTCAGGACA	GTAGCCCTTCTAATTCTCGG
UBC	CTGGGATACCATCCAGAACATC	CTCAAGTGTCCTTCCAGCATAG
RPL32	CCGCCACCTCTCTCTTTATTT	GCGCTTCTTGACAATCTTCTTG

2.9. Tissue-Specific Expression of LgDGATs

The NCBI database (https://www.ncbi.nlm.nih.gov/sra/) (accessed on 9 May 2023) provided the transcriptome information for *L. glauca* in five different tissues, including the sarcocarps, roots, leaves, stems, and seeds (accession number: SRX591256). The expression of heat maps was generated using the HeatMap program in TBtools software based on the transcriptome data.

3. Results

3.1. Identification of DGAT Members in L. glauca

Fifteen *DGAT* candidates (Table 2) were identified in *L. glauca* through Blastp and hmmer searches and domain analysis. Among them, one belonged to the *DGAT1* subfamily, and eight belonged to the *DGAT2* subfamily, while each subfamily of the *WSD* and *DGAT3* consisted of three members. Tables S1 and S2, respectively, contains the protein and gene sequences.

Table 2. Information on *LgDGAT*s in *L. glauca*.

Gene ID	Accession Number	AA	Molecular Weight	PI	Aliphatic Index	GRAVY	Predicted Location(s)	Transmembrane Domain
LgDGAT1	*Lg06G6989*	543	61,266.01	7.14	91.84	0.129	Endoplasmic reticulum	YES
LgDGAT2.1	*Lg05G6132*	292	32,678.24	9.28	95.72	0.189	Endoplasmic reticulum	NO
LgDGAT2.2	*Lg05G3126*	347	39,417.38	9.33	96.89	0.165	Endoplasmic reticulum	YES
LgDGAT2.3	*Lg05G3163*	349	39,622.65	9.33	96.33	0.175	Endoplasmic reticulum	YES
LgDGAT2.4	*Lg06G6636*	340	38,598.36	9.26	101.79	0.293	Endoplasmic reticulum	YES
LgDGAT2.5	*Lg08G2897*	304	33,914.54	5.23	85.89	−0.221	Endoplasmic reticulum	NO
LgDGAT2.6	*Lg10G4262*	279	30,661.56	8.86	82.15	0.146	Cell membrane	YES
LgDGAT2.7	*Lg03G1073*	486	55,057.85	8.64	98.27	−0.134	Endoplasmic reticulum	NO
LgDGAT2.8	*Lg03G1089*	1428	160,137.89	7.06	93.77	−0.132	Endoplasmic reticulum	NO
LgDGAT3.1	*Lg03G163*	90	9049.4	6.21	72.56	−0.11	Cell wall	NO
LgDGAT3.2	*Lg03G198*	259	27,851.62	8.58	73.13	−0.557	Nucleus	NO
LgDGAT3.3	*Lg06G3301*	360	38,915.39	5.68	66.89	−0.399	Nucleus	NO
LgWSD1	*Lg10G479*	168	18,727.96	8.72	96.37	0.083	Nucleus	NO
LgWSD2	*Lg10G489*	399	44,459.4	5.86	100.13	−0.026	Chloroplast	NO
LgWSD3	*Lg11G2666*	385	43,035.94	8.47	94.21	−0.023	Chloroplast	NO

Note: AA, PI, and GRAVY, respectively, indicate number of amino acids, theoretical isoelectric point, and average hydrophilicity of the protein.

Analysis of the *LgDGATs'* characteristics (Table 2) revealed that their length was between 90 and 1428 amino acids, their molecular weights were between 9.05 and 160.14 kDa, and their aliphatic indices were between 72.56 and 101.79. The theoretical isoelectric of these LgDGATs ranged from 5.23 to 9.33, and most were basic proteins. The grand average of hydropathicity was −0.557~0.293, of which *LgDGAT1*, *LgDGAT2.1*, *LgDGAT2.2*, *LgDGAT2.3*, *LgDGAT2.4*, *LgDGAT2.6*, and *LgWSD1* were classified as hydrophobic proteins. Subcellular localization analysis indicated that eight genes (*LgDGAT1*, *LgDGAT2.1*, *LgDGAT2.2*, *LgDGAT2.3*, *LgDGAT2.4*, *LgDGAT2.5*, *LgDGAT2.7*, and *LgDGAT2.8*) were located in the endoplasmic reticulum, three genes (*LgDGAT3.2*, *LgDGAT3.3*, and *LgWSD1*) were located in the nucleus, and two genes (*LgWSD2* and *LgWSD3*) were located in the chloroplast. *LgDGAT2.6* and *LgDGAT3.1* were found in cell membranes and cell walls, respectively. Furthermore, the analysis of transmembrane domains analysis showed that *LgDGAT1*, *LgDGAT2.2*, *LgDGAT2.3*, *LgDGAT2.4*, and *LgDGAT2.6* possessed transmembrane regions, while the remaining *LgDGAT* proteins had no transmembrane structures detected.

3.2. Phylogenetic Analysis of LgDGATs

The phylogenetic tree (Figure 1) constructed by the 50 DGATs from *L. glauca*, *A. thaliana*, *O. sativa*, *Z. mays*, *G. max*, and *B. napus* displayed that these proteins were clustered into four clades, DGAT1, DGAT2, DGAT3, and WSD. Further analysis indicated a close relationship between DGAT2 and DGAT3. Within the WSD clade, *LgWSD1* and *LgWSD2* were clustered together, suggesting that they possess similar and distinct functions. In the DGAT3 clade, *LgDGAT3.1*, *LgDGAT3.2*, and *LgDGAT3.3* were hypothesized to have functions similar to DGAT3 in *A. thaliana* and *B. napus*. Similarly, *LgDGAT1* was proposed to have more similar functions as DGAT1 in *O. sativa* and *Z. mays*. In the DGAT2 clade, eight *LgDGATs* (2.1 to 2.8) were clustered together, implying the presence of numerous redundant genes in DGAT2 due to gene replication during evolution.

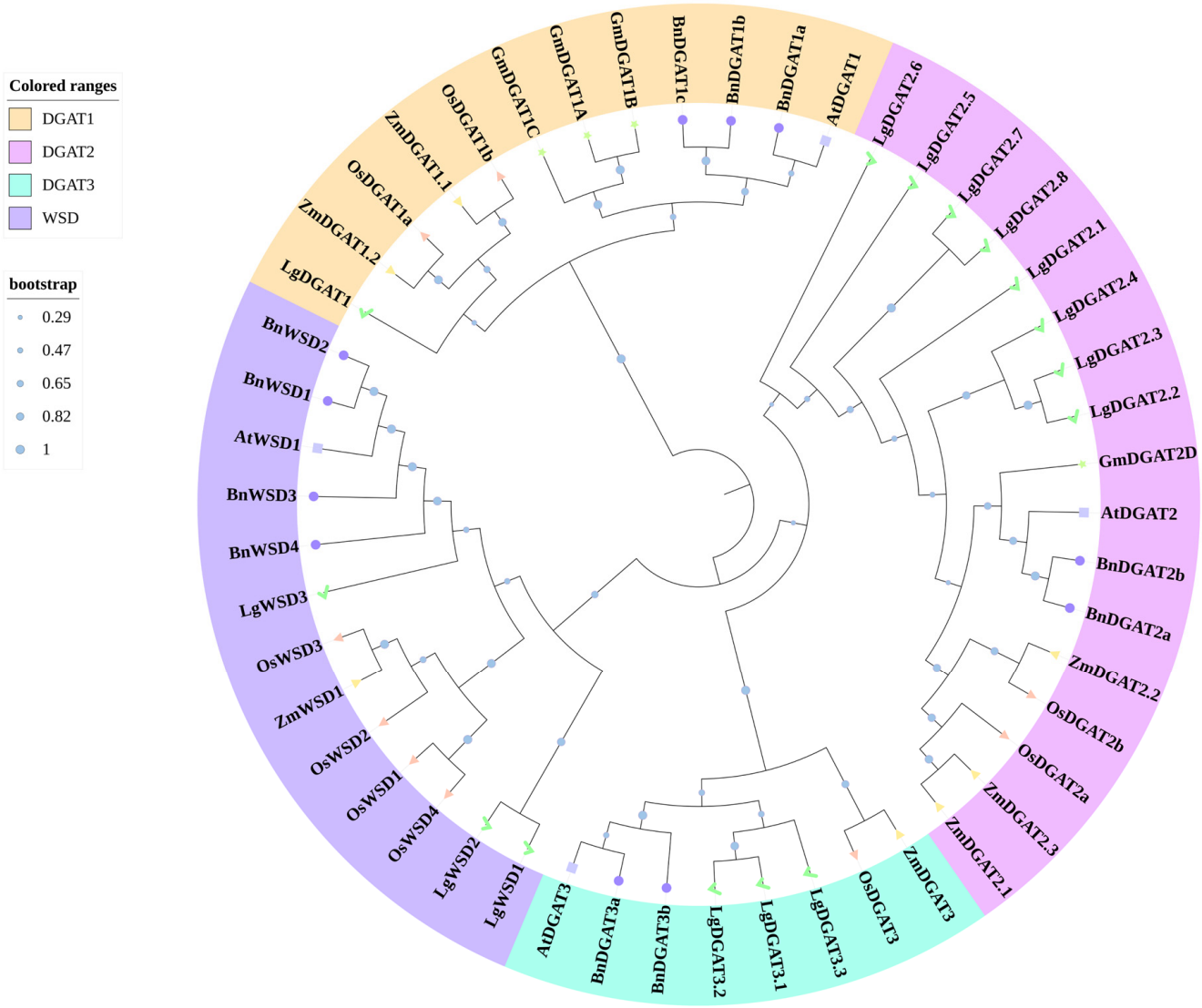

Figure 1. Phylogenetic tree of proteins from the DGAT family. Fifty DGATs of *Lindera glauca* (Lg), *Arabidopsis thaliana* (At), *Oryza sativa* (Os), *Zea mays* (Zm), *Glycine max* (Gm), and *Brassica napus* (Bn) are included in this tree. Distinct colors are used to designate distinct groupings of DGAT proteins. Each species of proteins is labeled with specific symbols.

3.3. Analysis of Conserved Motifs and Gene Structure of LgDGATs

The *LgDGAT* sequences were subjected to conservative motif prediction using the MEME online tool. The results indicated significant differences among different subfamilies (Figure 2B). Motif 1 was present in all members of the *LgDGAT2* subfamily, while motifs 6 and 14 were present in all *LgDGAT3* subfamily members. Motifs 8 and 9 were unique to the *LgWSD* subfamily and absent in other subfamilies. The *LgDGAT1* contained motifs 16 and 17, also found in the DGAT2 subfamily. Members within the same subfamily exhibited same or identical motif distributions, distinguishing them from other subfamilies. This finding suggested that genes in the same subfamily probably have similar roles, but genes in separate subfamilies have different roles. Moreover, the motif characteristics of each subfamily suggested that the *LgDGAT2* subfamily may have more complex functions than the other three subfamilies.

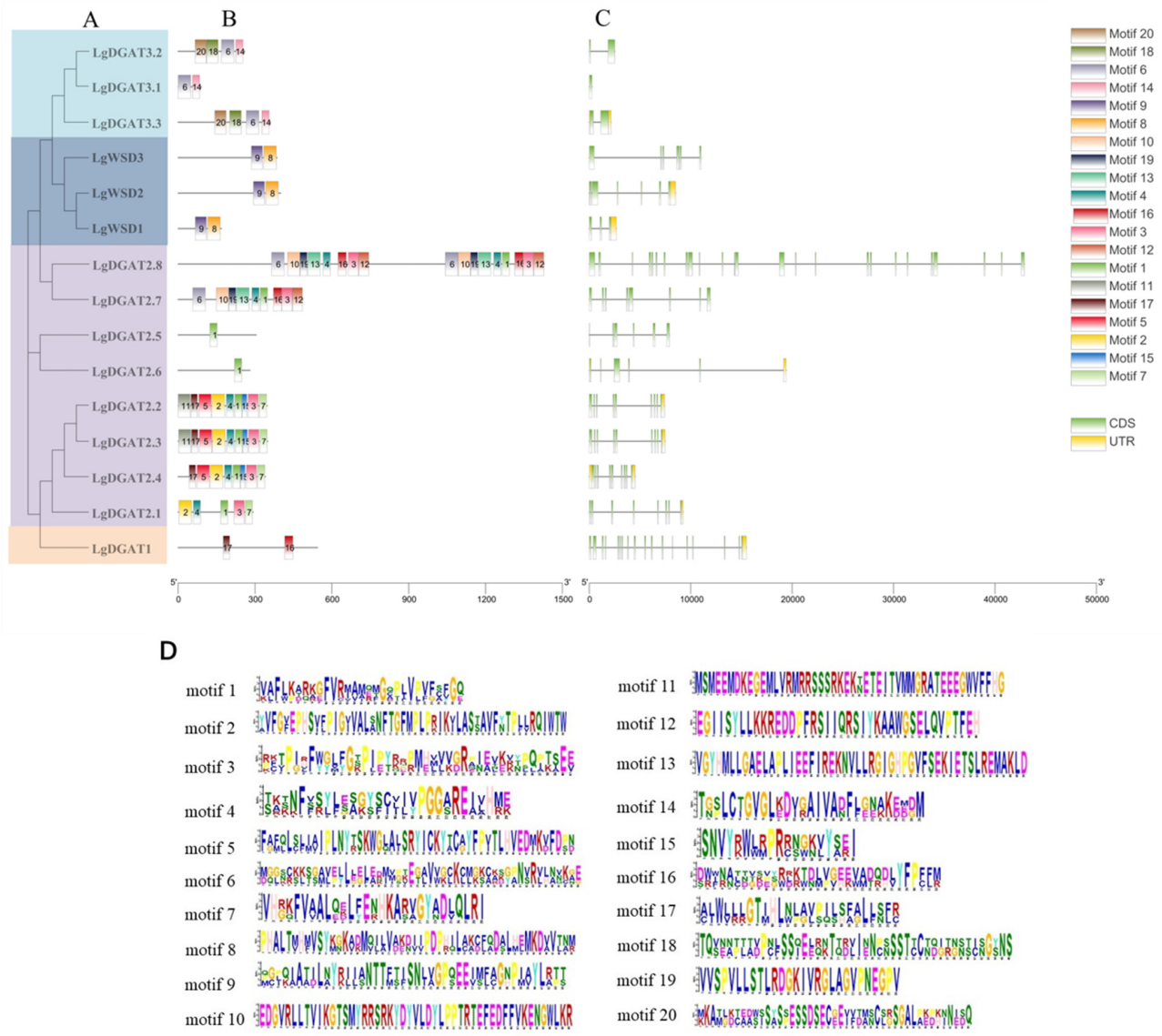

Figure 2. Phylogenetic relationships, gene structures and conserved motifs of the *LgDGAT* family. (**A**) Phylogenetic tree of *LgDGATs*. Different subfamily groupings are in different colors. (**B**) Conserved motifs of *LgDGATs*. Different motifs are represented by specific colors. (**C**) Gene structure of *LgDGATs*. Untranslated regions, introns, and exons are each denoted by a yellow box, black line, and green box, respectively. (**D**) Conserved motif logos of *LgDGATs*.

Four subfamilies of *LgDGATs* indicated distinct gene structures (Figure 2C). The *LgDGAT1* subfamily had 18 exons, while the *LgWSD* subfamily mainly consisted of three to six exons. The *LgDGAT3* subfamily had 1 to 2 exons, and the *LgDGAT2* subfamily exhibited a range of 6 to 9 exons, except the *LgDGAT2.8* had more than 20 exons. Notably, *LgDGAT2.8* possessed over 1000 amino acids, making it longer than other genes. This finding suggested that the length of this subfamily's genes and the number of exons may have increased due to gene evolution.

3.4. Cis-Acting Elements in LgDGAT Promoters

The potential regulatory mechanisms of *LgDGATs* were analyzed using PlantCARE database with 2000 bp upstream sequences (Figure 3). Four *cis*-acting elements were present in the promoter regions: plant hormone responsiveness, abiotic and biological stress, plant growth and development, and light response.

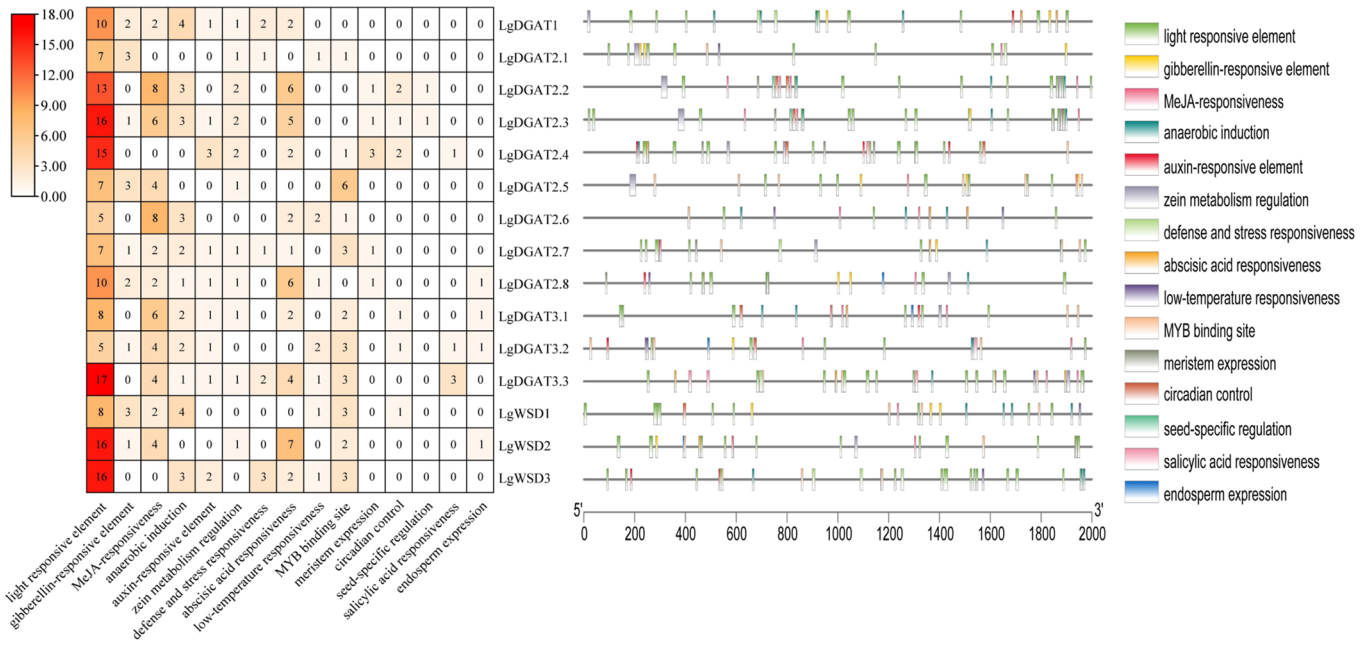

Figure 3. Distribution and number of *cis*-acting elements in the promoter region of *LgDGATs*. Different promoter elements are represented by different colored boxes.

Among all *LgDGATs*, *LgDGAT2.3*, *LgDGAT2.7*, *LgDGAT2.8*, *LgDGAT3.2*, and *LgDGAT3.3* contained the most amounts of *cis*-acting elements (10 elements), while *LgDGAT2.5* contained the fewest (5 elements). All *LgDGAT* promoters contained light-responsive elements. Regarding composition type specificity, most *LgDGAT* promoters contained MeJA-responsiveness, anaerobic induction, zein metabolism regulation, abscisic acid responsiveness, and MYB binding site elements. Approximately half of the *LgDGAT* promoters contained gibberellin-responsive element, auxin-responsive element, low-temperature responsiveness, and circadian control elements. Defense and stress-responsive elements were present in the promoters of *LgDGAT1*, *LgDGAT2.1*, *LgDGAT2.7*, *LgDGAT3.3*, and *LgWSD3*. Meristem expression elements were found in *LgDGAT2.2*, *LgDGAT2.3*, *LgDGAT2.4*, *LgDGAT2.7*, and *LgDGAT2.8*. Seed-specific regulation elements were present in *LgDGAT2.2* and *LgDGAT2.3*, while salicylic acid responsiveness elements were found in *LgDGAT2.4*, *LgDGAT3.2*, and *LgDGAT3.3*. Endosperm expression elements were detected in *LgDGAT2.8*, *LgDGAT3.1*, *LgDGAT3.2*, and *LgWSD2*.

3.5. Chromosomal Localization, Gene Duplication, and Genome Synteny of LgDGATs

Based on genomic annotation data, distribution maps of 15 *LgDGATs* in the chromosomes were created (Figure 4), illustrating the positions of each gene on various chromosomes. The distribution of these genes was as follows: one gene each on chromosomes 8 and 11, three genes each on chromosomes 5, 6, and 10, and four on chromosome 3. Two gene duplication events were uncovered, *LgDGAT2.1*/*LgDGAT2.2* and *LgDGAT2.2*/*LgDGAT2.3* (Figure 5, Table 2). Both duplicate gene pairs resulted from segmental duplication events, with no tandem duplication events observed among *LgDGATs*.

The *Ka*/*Ks* ratios of the two pair of paralogous genes were all less than 1.0, indicating the occurrence of purifying selection. This finding suggested that *LgDGATs* have undergone evolutionary conservation, contributing to maintenance of functional stability. In terms of divergence time, the *LgDGAT2.1*/*LgDGAT2.2* pair exhibited an earlier divergence time of 109.81 Mya, whereas divergence time of the *LgDGAT2.2*/*LgDGAT2.3* pair was only 0.67 Mya (Table 3). Furthermore, a collinearity analysis of *DGATs* (Figure 6) from *L. glauca*, *A. thaliana*, and *O. sativa* indicated that *LgWSD3* exhibited synteny with one *AtDGAT* (*AT5G53380.1*); *LgDGAT3.1* and *LgDGAT3.2* both exhibited synteny with one *OsDGAT*

(*OsKitaake05g027500.1*), suggesting that the *DGATs* of *L. glauca*, *A. thaliana*, and *O. sativa* had undergone dramatic evolutionary changes.

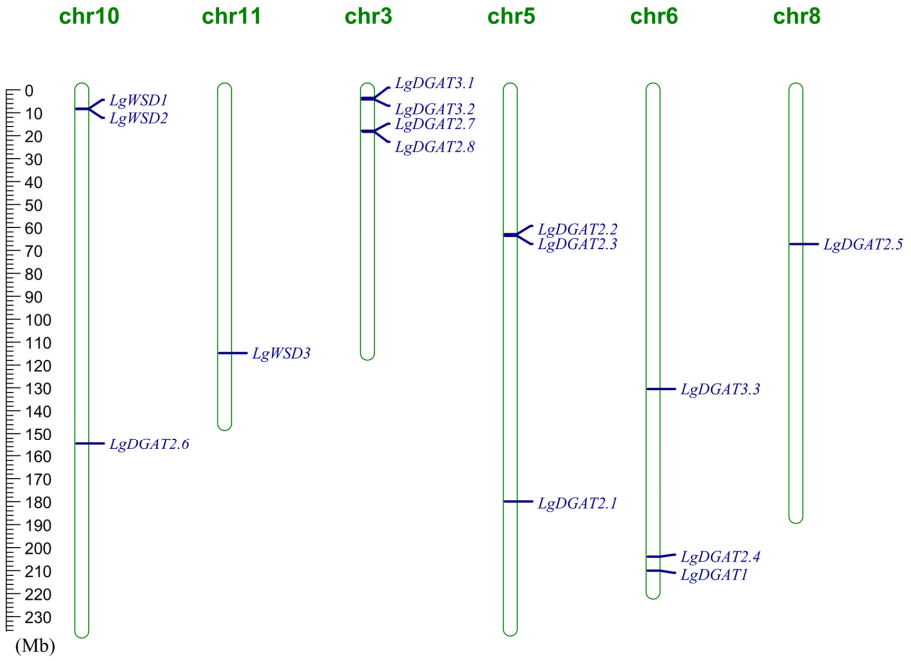

Figure 4. Chromosomal locations of *DGAT* genes in *L. glauca*.

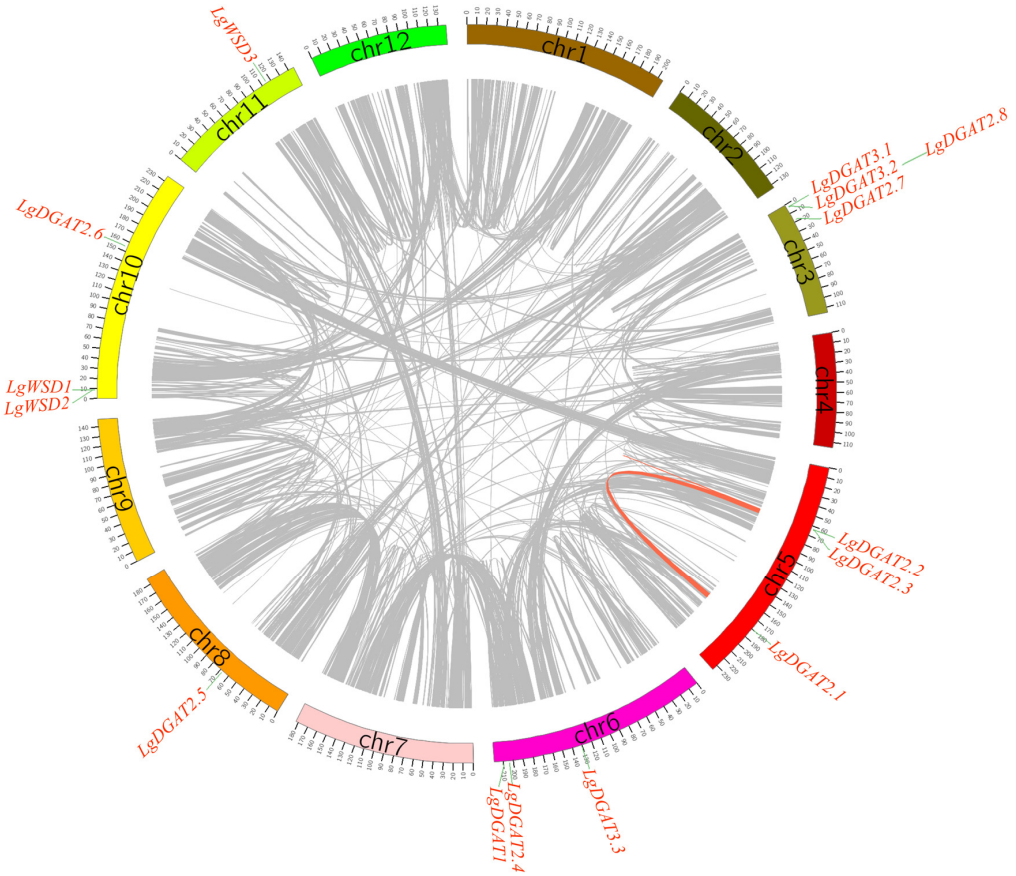

Figure 5. Collinearity analysis of *LgDGATs* in *L. glauca* genome. All of the genome's collinear blocks are shown by gray lines, while gene pairs with duplication events are represented by red lines.

Table 3. Gene duplication events and divergence time between paralogous pairs of *LgDGATs*.

Duplicated Gene 1	Duplicated Gene 2	*Ka*	*Ks*	*Ka*/*Ks*	Duplicated Type	Selective Type	Divergence Time (Mya)
LgDGAT2.2	*LgDGAT2.1*	0.223508	0.663243	0.336993	WGD or Segmental	Purifying	109.808444
LgDGAT2.2	*LgDGAT2.3*	0.001261	0.00406	0.310504	WGD or Segmental	Purifying	0.672185

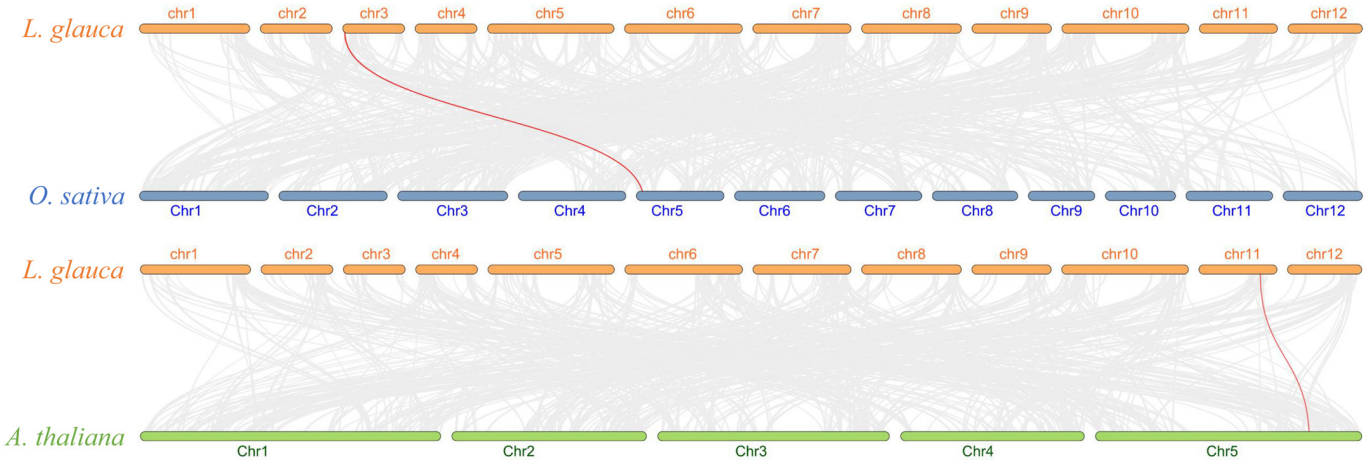

Figure 6. Collinearity analysis of DGATs among *L. glauca*, *O. sativa*, and *A. thaliana*. *LgDGATs*, *OsDGATs*, and *AtDGATs* are represented by orange, blue, and green, respectively. The gray lines in the background represent the collinear blocks identified in the genomes of *O. sativa*, *L. glauca*, and *A. thaliana*. Orange lines indicate the *DGAT* gene pairs.

3.6. Differential Expression Levels of LgDGAT Genes in Developing Fruit

L. glauca fruits (LGF) have emerged as a novel resource in China, possessing industrial and medicinal value due to their rich content of terpenoids and oil [29]. The biosynthesis and accumulation of oil in LGF may be regulated by certain genes, thereby influencing fruit growth and development. Hence, we systematically studied the expression of *LgDGATs* during fruit development stages (fruits at 60, 90, and 150 DAF) and identified specific genes that may regulate oil biosynthesis and accumulation in fruits (Figure 7A).

Expression analysis was performed for nine *LgDGATs* detected at three developmental stages: 60, 90, and 150 DAF. All nine genes exhibited expression throughout the entire fruit development process. During fruit development, *LgDGAT2.2*, *LgDGAT2.3*, and *LgDGAT3.3* showed similar expression patterns, with low expression levels at 60 and 90 DAF, reaching the lowest point at 90 DAF, followed by a significantly increase at 150 DAF. The expression level of *LgDGAT1* displayed an increasing trend, while *LgDGAT2.1* exhibited relatively stable and high expression levels, suggesting their potential involvement in TAG biosynthesis in fruits. *LgWSD1* and *LgWSD2* exhibited similar expression patterns, with a decrease followed by an increase in expression, peaking at 60 DAF. Conversely, *LgDGAT2.4* and *LgDGAT2.6* showed lower expression levels during fruit development, indicating their limited role in TAG accumulation in LGF. The qRT-PCR analysis was performed on randomly selected fruits at 90 DAF. The expression of nine genes was roughly consistent with the transcriptome data, which proved the accuracy of the transcriptome data.

3.7. Analysis of Expression Patterns of LgDGATs in Different Plant Tissues

Nine genes were found to have an expression when *LgDGATs* were examined for expression across various tissues, according to data retrieved from the NCBI database, while the other genes were not.

Their relative expression levels in seeds and stems were generally low (Figure 8). *LgDGAT1*, *LgDGAT2.2*, *LgDGAT2.3*, and *LgDGAT2.1* exhibited peak expression in the sarcocarps and low expression levels in leaves. *LgDGAT2.4*, *LgWSD1*, and *LgWSD2* showed peak

levels in leaves and low sarcocarps expression. *LgDGAT2.6* and *LgDGAT3.3* exhibited peak expression in roots. These results indicate distinct main expression sites for each *LgDGAT*, highlighting their functional specialization and close coordination. Similar expression patterns among these genes within the same subfamily were observed, such as *LgDGAT2.2* and *LgDGAT2.3*, and *LgWSD1* and *LgWSD2*.

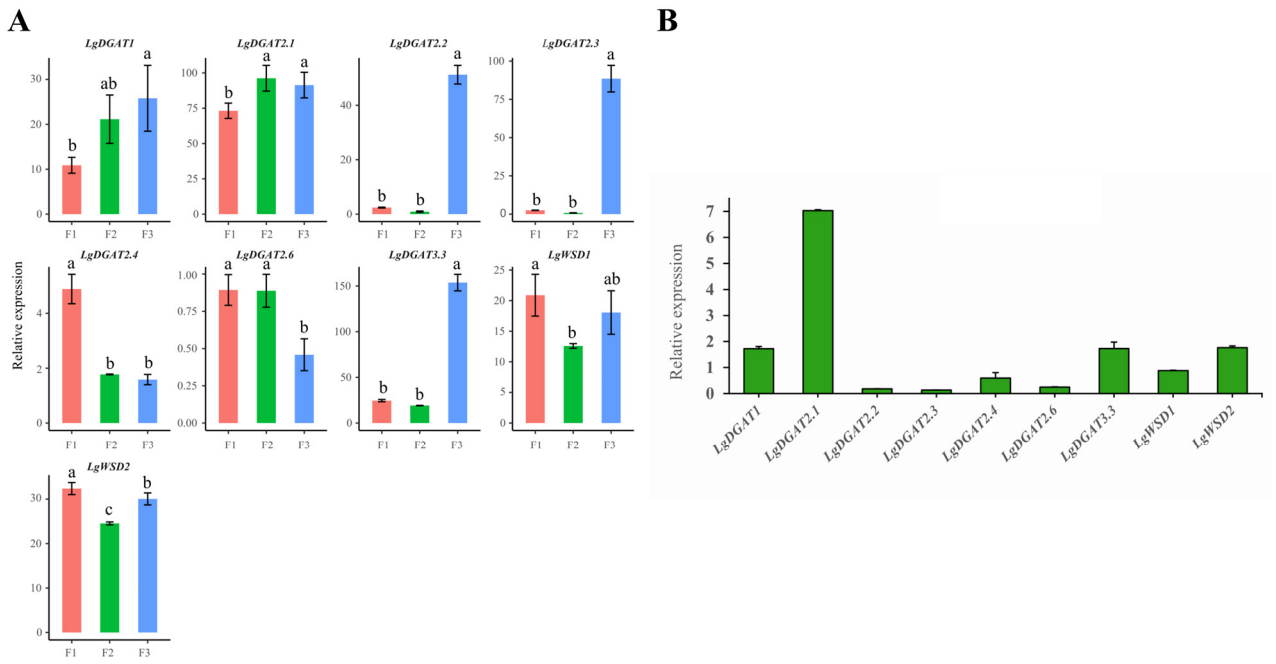

Figure 7. *LgDGATs'* expression patterns in developing fruit. (**A**) Expression analysis of nine *LgDGAT* genes during fruit development. F1, F2, and F3 indicate fruits at 60, 90, and 150 DAF, respectively. Data are indicated as means ± standard deviation (SD) from three samples. With the Duncan approach, lowercase letters above the bars demonstrate a significant difference ($p < 0.05$). (**B**) Gene expression data of nine *LgDGATs* in fruits at 90 DAF obtained via qRT-PCR analysis. Both *RPL32e* and *UBC* genes were used as the internal controls.

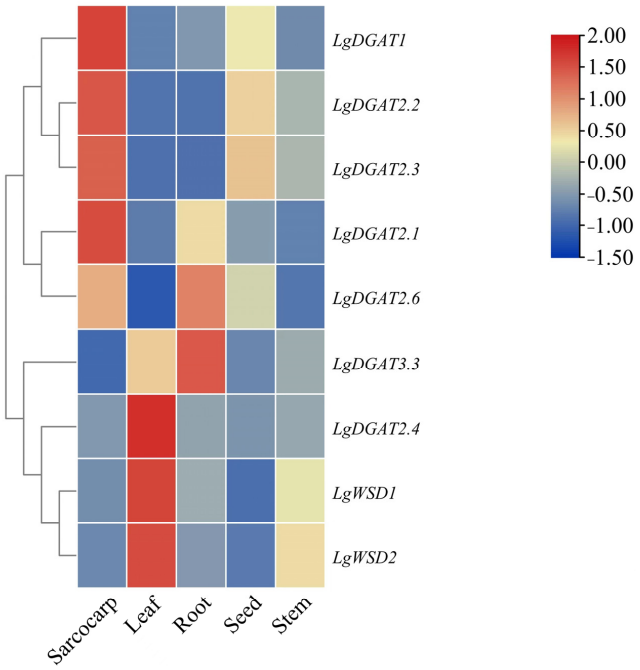

Figure 8. Relative patterns of *LgDGATs'* expression in the various tissues of *L. glauca*.

4. Discussion

L. glauca is known for its high oil content, surpassing that of conventional oil plants [49]. Apart from its edible applications, *L. glauca* oil derived from fruits or seeds has diverse industrial applications, such as in soaps, surfactants, and lubricants [32–34]. Mature *L. glauca* seeds have an oil content ranging from between 42.0% and 53.0% [50,51]. The biosynthesis of TAG, the primary oil component in plants, occurs in the endoplasmic reticulum through the catalysis action of multiple enzymes [52,53], with DGAT being the only rate-limiting enzyme for TAG biosynthesis [4]. The role of this enzyme in oil biosynthesis has been extensively studied in various plants [54–59], and overexpression of *DGATs* has been shown to enhance vegetable oils yield and quality [18]. However, no relevant report regarding the *LgDGATs* family exists. Using a bioinformatics method, we thoroughly analyzed *LgDGATs* in this study, encompassing phylogenetic evolution, gene structure, and gene expression, thus establishing a foundation for future investigations on improving *L. glauca* oil content.

We retrieved 15 *LgDGATs* from the *L. glauca* genome via aligning homologous sequences. Their number exceeds that of soybean (10), *Arabidopsis* (14), rice (5), and maize (5) [60,61]. The expansion of *LgDGAT* counts may reflect the evolution of *L. glauca* to adapt to its environment. The identified *LgDGAT*s were categorized into four subgroups: *LgDGAT1* (one gene), *LgDGAT2* (eight genes), *LgDGAT3* (three genes), and *LgWSD* (three genes). Exon–intron numbers and conserved motifs were similar among genes belonging to the same subfamily. However, gene structure and conserved motifs varied significantly among different subfamilies, indicating diverse biological functions within the same subfamily. Even though intron insertion or deletion aids in genome evolution [62], our results showed that not all *LgDGATs* lost introns equally, especially *LgDGAT2.8*. Recent studies have associated intron loss with genome reduction, suggesting that the number of introns primarily reflects the rate of evolution, with slower-evolving genes retaining more ancestral introns [63,64]. This diversity in *LgDGATs'* evolution was observed. Evolutionary analysis indicated that the members of four *LgDGAT* subfamilies were distributed across multiple monocotyledonous and dicotyledonous plants, forming distinct clusters. This finding suggests that the differentiation of these subfamilies predates species divergence or, akin to *DGAT1* and *DGAT2*, has an independent origin [65], consistent with previous research findings [66].

Previous research indicated that *DGAT1* and *DGAT2* were transmembrane proteins in different endoplasmic reticulum subdomains [67]. In this study, all *LgDGAT1* and *LgDGAT2s*, except *LgDGAT2.6*, were localized in the endoplasmic reticulum. Based on hydrophobicity index, subcellular localization, and transmembrane prediction, *LgDGAT1*, *LgDGAT2.2*, *LgDGAT2.3*, and *LgDGAT2.4* were identified as endoplasmic reticulum membrane proteins. Homologous genes derived from repetitive events often exhibit similar expression patterns [68]. Two pairs of fragment duplicates were found in *LgDGATs*, in which *LgDGAT2.2* and *LgDGAT2.3* had similar gene structures and conserved motifs and had similar expression patterns in different tissues and fruit development.

Further investigation indicated that these duplicated genes had a *Ka*/*Ks* ratio of less than 1.0, indicating purifying selection. Our findings support earlier evidence that the *DGAT* family may participate in abiotic stress responses, such as plant stress and low temperature, and contribute to TAG biosynthesis [69]. Plant adversity induces changes in membrane fluidity, and fatty acids were associated with membrane fluidity [70]. Most *LgDGATs* promoter contained MYB binding sites, suggesting the potential regulation of *LgDGATs* by MYB transcription factors. Additionally, we identified the *cis*-acting elements responsive to various phytohormones, including MeJA, GA, IAA, and ABA. ABA is widely recognized for its significant role in plants responses to biotic and abiotic stressors [71]. The ABA-responsive element was present in almost all *LgDGAT*s, implying a potential association with the response to abiotic stress. The photoresponsive element was present in all *LgDGATs*, and thus we speculated a potential association between *LgDGATs* and photosynthesis.

While *DGATs* primarily participate in oil accumulation, they are also involved in lipid metabolism during biological processes such as seed germination, seedling development and leaf senescence [72]. Consequently, *DGATs* are expected to be expressed in various tissues, including seeds, flowers, and leaves, albeit with tissue-specific expression levels. For instance, *DGAT1* in *Tropaeolum majus* is exclusively expressed in developing seeds [59], and *DGAT1* expression in rosette increases with leaf senescence [73]. Tung tree *DGAT1* shows minimal expression differences among organs, whereas *DGAT2* is highly expressed in developing seeds [56]. *AtDGAT1* exhibits high expression in developing *Arabidopsis* seeds, correlating with TAG accumulation [74]. In this study, nine expressed *LgDGATs* were identified via the transcriptome data in different *L. glauca* tissues obtained from the NCBI database and fruits during three developmental stages sequenced by us. These genes include *LgDGAT1*, *LgDGAT2.1*, *LgDGAT2.2*, *LgDGAT2.3*, *LgDGAT2.4*, *LgDGAT2.6*, *LgDGAT3.3*, *LgWSD1*, and *LgWSD2*. The remaining six *LgDGATs* were not detected in either transcriptome data, suggesting that they may be pseudogenes or expressed at shallow levels during these periods. In this study, *LgDGAT2.1* was significantly expressed during fruit development, and fruits at 150 DAF had high *LgDGAT2.2*, *LgDGAT2.3*, and *LgDGAT3.3* expression. These genes may play pivotal roles in oil accumulation in developing fruits. However, the *LgWSD* subfamilies were mainly expressed in stems, leaves, and other organs, consistent with the study on sunflower [75]. We hypothesized that the *LgWSD* subfamilies may involve lipid accumulation and cuticle wax formation in these tissues. Plant cuticle prevents excessive water loss, resists ultraviolet radiation, and protects against diseases and pests [76]. *AtWSD1* has been implicated in epidermal wax synthesis in stems and is vital for *Arabidopsis*' adaptation to drought stress [19,20]. *AtWSD11* (*FOP1*) exhibits high expression in *Arabidopsis* flowers, and its encoded product may act as a lubricant to enable uninhibited growth of petals as they extend between sepals and anthers [77]. The distinct tissue expression patterns of the four *LgDGAT* subfamilies indicate functional divergence among *LgDGATs*, suggesting a finely regulated process of oil accumulation in *L. glauca*.

5. Conclusions

In this study, 15 *LgDGATs* were identified in the *L. glauca* genome through bioinformatics analysis. The *LgDGATs* were comprehensively analyzed for physicochemical properties, chromosome localization, conserved motifs, gene structure, evolutionary relationship and *cis*-acting elements. Based on the similarities between these genes' structures and functions, they were divided into four groups. The *cis*-acting components in their promoter region were linked to plant hormone signaling, plant growth and development, abiotic and biological stress responses, and light responsiveness. According to transcriptome data, nine *LgDGATs* were among the identified genes and showed measurable expression levels in three stages of fruit development and different tissues. Expression pattern analysis indicated the significant involvement of *LgDGAT2.1* in TAC accumulation in the LFG. Our results provide valuable insights and data for future investigations on the functional characterization of *LgDGATs* and offer novel candidate genes for utilizing *L. glauca* resources.

Supplementary Materials: The following supporting information can be downloaded at https://www.mdpi.com/article/10.3390/f14081633/s1, Table S1: The protein sequences of *LgDGATs*; Table S2: The gene sequences of *LgDGATs*.

Author Contributions: Conceptualization, B.X.; methodology, X.B.; software, X.B.; validation, Y.Y.; resources, B.X.; data curation, L.X.; writing—original draft preparation, X.B.; writing—review and editing, B.X.; visualization, Q.L.; supervision, B.X.; project administration, X.B.; funding acquisition, B.X. All authors have read and agreed to the published version of the manuscript.

Funding: This research was funded by the National Natural Science Foundation of China (31900272; 32260086), National Guidance of Local Science and Technology Development Fund of China ([2023]009), Guizhou Science and Technology Plan Project (Qiankehe Basics–ZK [2021] General 151 and Qiankehe Support [2022] General 057), Young Talents Program of Guizhou Provincial Department of Education (Qianjiaohe Basics–KY [2021]), Cultivation Project of Guizhou University (Gzu. 2020 No. 65), and Guizhou Provincial Postgraduate Research Fund (YJSKYJJ [2021] 005).

Data Availability Statement: The data that support the findings of this study are openly available in the NCBI database (https://www.ncbi.nlm.nih.gov/sra/) (accessed on 1 June 2023). The accession number is SRX591256 and PRJNA977679.

Conflicts of Interest: The authors declare no conflict of interest.

References

1. Lung, S.C.; Weselake, R.J. Diacylglycerol acyltransferase: A key mediator of plant triacylglycerol synthesis. *Lipids* **2006**, *41*, 1073–1088. [CrossRef]
2. Liu, Q.; Siloto, R.M.P.; Lehner, R.; Stone, S.J.; Weselake, R.J. Acy1–CoA: Diacylglycerol acyltransferase: Molecular biology, biochemistry and biotechnology. *Prog. Lipid Res.* **2012**, *51*, 350–377. [CrossRef] [PubMed]
3. Kennedy, E.P.; Weiss, S.B. Function of cytidine coenzymes in the biosynthesis of phospholipides. *J. Biol. Chem.* **1956**, *222*, 193–213. [CrossRef] [PubMed]
4. Chapman, K.D.; Ohlrogge, J.B. Compartmentation of triacylglycerol accumulation in plants. *J. Biol. Chem.* **2012**, *287*, 2288–2294. [CrossRef] [PubMed]
5. Hernández, M.L.; Whitehead, L.; He, Z.; Gazda, V.; Gilday, A.; Kozhevnikova, E.; Vaistij, F.; Larson, T.R.; Graham, I.A. A cytosolic acyltransferase contributes to triacylglycerol synthesis in sucrose–rescued Arabidopsis seed oil catabolism mutants. *Plant Physiol.* **2012**, *160*, 215–225. [CrossRef] [PubMed]
6. Kalscheuer, R.; Steinbüchel, A. A novel bifunctional wax ester synthase/acyl–CoA: Diacylglycerol acyltransferase mediates wax ester and triacylglycerol biosynthesis in *Acinetobacter calcoaceticus* ADP1. *J. Biol. Chem.* **2003**, *278*, 8075–8082. [CrossRef] [PubMed]
7. Nykiforuk, C.L.; Furukawa-Stoffer, T.L.; Huff, P.W.; Sarna, M.; Laroche, A.; Moloney, M.M.; Weselake, R.J. Characterization of cDNAs encoding diacylglycerol acyltransferase from cultures of Brassica napus and sucrose–mediated induction of enzyme biosynthesis. *Biochim. Biophys. Acta* **2002**, *1580*, 95–109. [CrossRef]
8. Zhang, F.Y.; Yang, M.F.; Xu, Y.N. Silencing of DGAT1 intobacco causes a reduction in seed oil content. *Plant Sci.* **2005**, *169*, 689–694. [CrossRef]
9. Lock, Y.Y.; Snyder, C.L.; Zhu, W.; Siloto, R.M.; Weselake, R.J.; Shah, S. Antisense suppression of type 1 diacylglycerol acyltransferase adversely affects plant development in *Brassica napus*. *Physiol. Plant* **2009**, *137*, 61–71. [CrossRef]
10. Zhang, M.; Fan, J.; Taylor, D.C.; Ohlrogge, J.B. *DGAT1* and *PDAT1* acyltransferases have overlapping functions in *Arabidopsis* triacylglycerol biosynthesis and are essential for normal pollen and seed development. *Plant Cell.* **2009**, *21*, 3885–3901. [CrossRef]
11. Zou, J.; Wei, Y.; Jako, C.; Kumar, A.; Selvaraj, G.; Taylor, D.C. The *Arabidopsis thaliana TAG1* mutant has a mutation in a diacylglycerol acyltransferase gene. *Plant J. Cell Mol. Biol.* **1999**, *19*, 645–653. [CrossRef] [PubMed]
12. Poirier, Y.; Ventre, G.; Caldelari, D. Increased flow of fatty acids toward beta– oxidation in developing seeds of Arabidopsis deficient in diacylglycerol acyltransferase activity or synthesizing medium–chain–length fatty acids. *Plant Physiol.* **1999**, *121*, 1359–1366. [CrossRef] [PubMed]
13. Andrianov, V.; Borisjuk, N.; Pogrebnyak, N.; Brinker, A.; Dixon, J.; Spitsin, S.; Flynn, J.; Matyszczuk, P.; Andryszak, K.; Laurelli, M.; et al. Tobacco as a production platform for biofuel: Overexpression of Arabidopsis DGAT and LEC2 genes increases accumulation and shifts the composition of lipids in green biomass. *Plant Biotechnol. J.* **2010**, *8*, 277–287. [CrossRef]
14. Lu, G.; Li, D.; Zhang, T.; Tang, X.; Lu, J.X.; Hu, Q.M.; Hu, T.M. Cloning and function analysis of a type 2 diacylglycerol acyltransferase (DGAT2) from *Perilla frutescens*. *Acta Agron. Sin.* **2020**, *46*, 1283–1290. [CrossRef]
15. Zhang, T.; He, H.; Xu, C.; Fu, Q.; Tao, Y.; Xu, R.; Xu, Z. Overexpression of Type 1 and 2 Diacylglycerol Acyltransferase Genes (*JcDGAT1* and *JcDGAT2*) Enhances Oil Production in the Woody Perennial Biofuel Plant *Jatropha curcas*. *Plants* **2021**, *10*, 699. [CrossRef] [PubMed]
16. Gao, Y.; Sun, Y.; Gao, H.L.; Xue, J.A.; Jia, X.Y.; Li, R.Z. Functional analysis of CEDGAT2–2 gene in Cyperus esculentus L. and cultivation of oil fuel–type tobacco. In Proceedings of the 19th Annual Conference of Crop Science Society of China, Wuhan, China, 8–9 November 2020; Crop Science Society of China: Wuhan, China, 2020; Volume 1.
17. Ayme, L.; Arragain, S.; Canonge, M.; Baud, S.; Touati, N.; Bimai, O.; Jagic, F.; Louis-Mondesir, C.; Briozzo, P.; Fontecave, M.; et al. Arabidopsis thaliana DGAT3 is a [2Fe–2S] protein involved in TAG biosynthesis. *Sci. Rep.* **2018**, *8*, 17254. [CrossRef]
18. Gao, H.L.; Gao, Y.; Zhang, F.; Liu, B.L.; Ji, C.L.; Xue, J.A.; Yuan, L.X.; Li, R.Z.; Sativa, C. Functional characterization of an novel acyl–CoA: Diacylglycerol acyltransferase 3–3 (CsDGAT3–3) gene from Camelina sativa. *Plant Sci.* **2021**, *303*, 110752. [CrossRef]
19. Li, F.; Wu, X.; Lam, P.; Bird, D.; Zheng, H.; Samuels, L.; Jetter, R.; Kunst, L. Identification of the wax ester synthase/acyl–coenzyme A: Diacylglycerol acyltransferase WSD1 required for stem wax ester biosynthesis in Arabidopsis. *Plant Physiol.* **2008**, *148*, 97–107. [CrossRef]

20. Patwari, P.; Salewski, V.; Gutbrod, K.; Kreszies, T.; Dresen-Scholz, B.; Peisker, H.; Steiner, U.; Meyer, A.J.; Schreiber, L.; Dormann, P. Surface wax esters contribute to drought tolerance in *Arabidopsis*. *Plant J.* **2019**, *98*, 727–744. [CrossRef]
21. Wang, Y.L.; Gao, X.M.; Yu, X.P.; Cheng, S.L.; Kong, L.H. Study on the resource and its utilizations of *Lindera glauca* in China. *Henan Sci.* **1994**, *12*, 331–334.
22. Seki, K.; Sasaki, T.; Haga, K.; Kaneko, R. Two methoxybutanolides from *Lindera glauca*. *Phytochemistry* **1994**, *36*, 949–951. [CrossRef]
23. Huh, G.W.; Park, J.H.; Kang, J.H.; Jeong, T.S.; Kang, H.C.; Baek, N.I. Flavonoids from *Lindera glauca* Blume as low–density lipoprotein oxidation inhibitors. *Nat. Prod. Res.* **2014**, *28*, 831–834. [CrossRef] [PubMed]
24. Dupont, Y.L. Evolution of apomixis as a strategy of colonization in the dioecious species *Lindera glauca* (Lauraceae). *Popul. Ecol.* **2002**, *44*, 293–297. [CrossRef]
25. Tsui, H.P.; Xia, Z.D.; Li, J.L. *Lauraceae and Hernandiaceae*; Li, H.W., Ed.; Flora of China Science Press: Beijing, China, 1982; Volume 31, pp. 393–394.
26. Tsui, H.P.; Werff, H. *Lauraceae and Hernandiaceae*; Li, H.W., Ed.; Flora of China Science Press: Beijing, China; Missouri Botanical Garden Press: St. Louis, MO, USA, 2008; Volume 7, pp. 146–147.
27. Huh, G.W.; Park, J.H.; Shrestha, S.; Lee, Y.H.; Ahn, E.M.; Kang, H.C.; Baek, N.I. Sterols from *Lindera glauca* Blume stem wood. *J. Appl. Biol. Chem.* **2011**, *54*, 309–312. [CrossRef]
28. Xiong, B.; Zhang, L.; Dong, S.; Zhang, Z. Population genetic structure and variability in *Lindera glauca* (Lauraceae) indicates low levels of genetic diversity and skewed sex ratios in natural populations in mainland China. *PeerJ* **2020**, *8*, 8304. [CrossRef]
29. Qi, J.; Xiong, B.; Ju, Y.X.; Hao, Q.; Zhang, Z.X. Study on fruit growth regularity and lipid accumulation of *Lindera glauca*. *Chinese Agri Sci Bull.* **2015**, *31*, 29–33.
30. Lin, Z.; An, J.; Wang, J.; Niu, J.; Ma, C.; Wang, L.; Yuan, G.; Shi, L.; Liu, L.; Zhang, J.; et al. Integrated analysis of 454 and Illumina transcriptomic sequencing characterizes carbon flux and energy source for fatty acid synthesis in developing *Lindera glauca* fruits for woody biodiesel. *Biotechnol. Biofuels* **2017**, *10*, 134. [CrossRef]
31. Zhu, B.; Hou, X.; Niu, J.; Li, P.; Fang, C.; Qiu, L.; Ha, D.; Zhang, Z.; Sun, J.; Li, Y.; et al. Volatile constituents from the fruits of *Lindera glauca* (Sieb. et Zucc.) with different maturities. *J. Essent. Oil Bear. Plants* **2016**, *19*, 926–935. [CrossRef]
32. Sun, H.L.; Wang, J.X.; Gu, X.Z.; Kang, W.Y. Analysis of volatile compounds from leaves and fruits of *Lindera glauca*. *Chin. J. Exp. Tradit. Med.* **2011**, *7*, 033.
33. Kim, K.H.; Moon, E.; Ha, K.; Suh, W.S.; Kim, H.H.; Kim, S.Y.; Choi, S.U.; Lee, K.R. Bioactive lignan constituents from the twigs of *Lindera glauca*. *Chem. Pharm. Bull.* **2014**, *62*, 1136–1140. [CrossRef]
34. Suh, W.S.; Kim, K.H.; Kim, H.K.; Choi, S.U.; Lee, K.R. Three new lignan derivatives from *Lindera glauca* (Siebold et Zucc.) Blume. *Helv. Chim. Acta* **2015**, *98*, 1087–1094. [CrossRef]
35. El-Gebali, S.; Mistry, J.; Bateman, A.; Eddy, S.R.; Luciani, A.; Potter, S.C.; Qureshi, M.; Richardson, L.J.; Salazar, G.A.; Smart, A.; et al. The Pfam protein families database in 2019. *Nucleic Acids Res.* **2019**, *47*, D427–D432. [CrossRef]
36. Johnson, L.S.; Eddy, S.R.; Portugaly, E. Hidden Markov model speed heuristic and iterative HMM search procedure. *BMC Bioinform.* **2010**, *11*, 431. [CrossRef] [PubMed]
37. Marchler-Bauer, A.; Bryant, S.H. CD–Search: Protein domain annotations on the fly. *Nucleic Acids Res.* **2004**, *32* (Suppl. S2), W327–W331. [CrossRef]
38. Garg, V.K.; Avashthi, H.; Tiwari, A.; Jain, P.A.; Ramkete, P.W.; Kayastha, A.M.; Singh, V.K. MFPPI–multi FASTA ProtParam interface. *Bio. Inf.* **2016**, *12*, 74–77. [CrossRef]
39. Krogh, A.; Larsson, B.; von Heijne, G.; Sonnhammer, E.L. Predicting transmembrane protein topology with a hidden Markov model: Application to complete genomes. *J. Mol. Biol.* **2001**, *305*, 567–580. [CrossRef] [PubMed]
40. Letunic, I.; Bork, P. Interactive tree of life (ITOL) v5: An online tool for phylogenetic tree displays and annotation. *Nucleic Acids Res.* **2021**, *49*, W293–W296. [CrossRef] [PubMed]
41. Bailey, T.L.; Boden, M.; Buske, F.A.; Frith, M.; Grant, C.E.; Clementi, L.; Ren, J.; Li, W.W.; Noble, W.S. MEME SUITE: Tools for motif discovery and searching. *Nucleic Acids Res.* **2009**, *37*, W202–W208. [CrossRef]
42. Chen, C.; Chen, H.; Zhang, Y.; Thomas, H.R.; Frank, M.H.; He, Y.; Xia, R. TBtools: An integrative toolkit developed for interactive analyses of big biological data. *Mol. Plant* **2020**, *13*, 1194–1202. [CrossRef]
43. Lescot, M.; Dehais, P.; Thijs, G.; Marchal, K.; Moreau, Y.; Van de Peer, Y.; Rouze, P.; Rombauts, S. PlantCARE, a database of plant cis-acting regulatory elements and a portal to tools for in silico analysis of promoter sequences. *Nucleic Acids Res.* **2002**, *30*, 325–327. [CrossRef]
44. Voorrips, R.E. MapChart: Software for the graphical presentation of linkage maps and QTLs. *J. Hered.* **2002**, *93*, 77–78. [CrossRef]
45. Wang, Y.; Tang, H.; Debarry, J.D.; Tan, X.; Li, J.; Wang, X.; Lee, T.H.; Jin, H.; Marler, B.; Guo, H.; et al. MCScanX: A toolkit for detection and evolutionary analysis of gene synteny and collinearity. *Nucleic Acids Res.* **2012**, *40*, e49. [CrossRef] [PubMed]
46. Krzywinski, M.; Schein, J.; Birol, I.; Connors, J.; Gascoyne, R.; Horsman, D.; Jones, S.J.; Marra, M.A. Circos: An information aesthetic for comparative genomics. *Genome Res.* **2009**, *19*, 1639–1645. [CrossRef] [PubMed]
47. Cui, L.; Wall, P.K.; Leebens-Mack, J.H.; Lindsay, B.G.; Soltis, D.E.; Doyle, J.J.; Soltis, P.S.; Carlson, J.E.; Arumuganathan, K.; Barakat, A.; et al. Widespread genome duplications throughout the history of flowering plants. *Genome Res.* **2006**, *16*, 738–749. [CrossRef] [PubMed]
48. Field, A. *Discovering Statistics Using IBM SPSS Statistics*; Sage Publications Ltd.: Thousand Oaks, CA, USA, 2013.

49. Wang, R.; Hanna, M.A.; Zhou, W.W.; Bhadury, P.S.; Chen, Q.; Song, B.A.; Yang, S. Production and selected fuel properties of biodiesel from promising non–edible oils: *Euphorbia lathyris* L., *Sapium sebiferum* L. and *Jatropha curcas* L. *Bioresour. Technol.* **2011**, *102*, 1194–1199. [CrossRef] [PubMed]
50. Qian, X.S.; Xiao, Z.C. Study and utilization of Lindera glauca in China. *Wild Plant Resour.* **1985**, *2*, 2–6.
51. Wang, J.P.; Meng, S.J.; Li, J.M. Fatty acid of oils of Lauraceae. *Acta Bot. Sin.* **1984**, *27*, 175–185.
52. Baud, S.; Lepiniec, L. Physiological and developmental regulation of seed oil production. *Prog. Lipid Res.* **2010**, *49*, 235–249. [CrossRef]
53. Barthole, G.; Lepiniec, L.; Rogowsky, P.M.; Baud, S. Controlling lipid accumulation in cereal grains. *Plant Sci.* **2012**, *185*, 33–39. [CrossRef]
54. Chen, B.; Wang, J.; Zhang, G.; Liu, J.; Manan, S.; Hu, H.; Zhao, J. Two types of soybean diacylglycerol acyltransferases are differentially involved in triacylglycerol biosynthesis and response to environmental stresses and hormones. *Sci. Rep.* **2016**, *6*, 28541. [CrossRef]
55. Li, R.; Hatanaka, T.; Yu, K.; Wu, Y.; Fukushige, H.; Hildebrand, D. Soybean oil biosynthesis: Role of diacylglycerol acyltransferases. *Funct. Integr. Genom.* **2013**, *13*, 99–113. [CrossRef] [PubMed]
56. Shockey, J.M.; Gidda, S.K.; Chapital, D.C.; Kuan, J.C.; Dhanoa, P.K.; Bland, J.M.; Rothstein, S.J.; Mullen, R.T.; Dyer, J.M. Tung tree DGAT1 and DGAT2 have nonredundant functions in triacylglycerol biosynthesis and are localized to different subdomains of the endoplasmic reticulum. *Plant Cell* **2006**, *18*, 2294–2313. [CrossRef]
57. Wang, H.; Zhang, J.; Gai, J.; Chen, S. Cloning and comparative analysis of the gene encoding diacylglycerol acyltransferase from wild type and cultivated soybean. *Theor. Appl. Genet.* **2006**, *112*, 1086–1097. [CrossRef] [PubMed]
58. Zheng, P.; Allen, W.B.; Roesler, K.; Williams, M.E.; Zhang, S.; Li, J.; Glassman, K.; Ranch, J.; Nubel, D.; Solawetz, W.; et al. A phenylalanine in DGAT is a key determinant of oil content and composition in maize. *Nat. Genet.* **2008**, *40*, 367–372. [CrossRef]
59. Xu, J.; Francis, T.; Mietkiewska, E.; Giblin, E.M.; Barton, D.L.; Zhang, Y.; Zhang, M.; Taylor, D.C. Cloning and characterization of an acyl–CoA–dependent diacylglycerol acyltransferase 1 (DGAT1) gene from *Tropaeolum majus*, and a study of the functional motifs of the DGAT protein using site–directed mutagenesis to modify enzyme activity and oil content. *Plant Biotechnol. J.* **2008**, *6*, 799–818. [CrossRef]
60. Zhao, J.; Bi, R.; Li, S.; Zhou, D.; Bai, Y.; Jing, G.; Zhang, K.; Zhang, W. Genome–wide analysis and functional characterization of Acyl–CoA: Diacylglycerol acyltransferase from soybean identify GmDGAT1A and 1B roles in oil synthesis in *Arabidopsis* seeds. *J. Plant Physiol.* **2019**, *242*, 153019. [CrossRef]
61. Yan, B.; Xu, X.; Gu, Y.; Zhao, Y.; Zhao, X.; He, L.; Zhao, C.; Li, Z.; Xu, J. Genome–wide characterization and expression profiling ofdiacylglycerol acyltransferase genes from maize. *Genome* **2018**, *61*, 735–743. [CrossRef]
62. Sharpton, T.J.; Neafsey, D.E.; Galagan, J.E.; Taylor, J.W. Mechanisms of intron gain and loss in *Cryptococcus*. *Genome Biol.* **2008**, *9*, R24. [CrossRef]
63. Lynch, M.; Richardson, A.O. The evolution of spliceosomal introns. *Curr. Opin. Genet. Dev.* **2002**, *12*, 701–710. [CrossRef] [PubMed]
64. Roy, S.W.; Gilbert, W. The evolution of spliceosomal introns: Patterns, puzzles and progress. *Nat. Rev. Genet.* **2006**, *7*, 211–221.
65. Turchetto-Zolet, A.C.; Maraschin, F.S.; de Morais, G.L.; Cagliari, A.; Andrade, C.M.; Margis-Pinheiro, M.; Margis, R. Evolution-aryview of acyl–CoA diacylglycerol acyltransferase (DGAT), a key enzyme in neutral lipid biosynthesis. *BMC Evol. Biol.* **2011**, *11*, 263. [CrossRef]
66. Turchetto-Zolet, A.C.; Christoff, A.P.; Kulcheski, F.R.; Loss-Morais, G.; Margis, R.; Margis-Pinheiro, M. Diversity and evolution of plant diacylglycerol acyltransferase (DGATs) unveiled by phylogenetic, gene structure and expression analyses. *Genet. Mol. Biol.* **2016**, *39*, 524–538. [CrossRef]
67. Bhatt-Wessel, B.; Jordan, T.W.; Miller, J.H.; Peng, L. Role of DGAT enzymes in triacylglycerol metabolism. *Arch. Biochem. Biophys.* **2018**, *655*, 1–11. [CrossRef] [PubMed]
68. Ganko, E.W.; Meyers, B.C.; Vision, T.J. Divergence in expression between duplicated genes in Arabidopsis. *Mol. Biol. Evol.* **2007**, *24*, 2298–2309. [CrossRef] [PubMed]
69. Singer, S.D.; Zou, J.; Weselake, R.J. Abiotic factors influence plant storage lipid accumulation and composition. *Plant Sci.* **2016**, *243*, 1–9. [CrossRef] [PubMed]
70. Young, D.Y.; Shachar-Hill, Y. Large fluxes of fatty acids from membranes to triacylglycerol and back during N–deprivation and recovery in Chlamydomonas. *Plant Physiol.* **2020**, *185*, 796–814. [CrossRef]
71. Chen, K.; Li, G.J.; Bressan, R.A.; Song, C.P.; Zhu, J.K.; Zhao, Y. Abscisic acid dynamics, signaling, and functions in plants. *J. Integr.Plant Biol.* **2020**, *62*, 25–54. [CrossRef]
72. Liu, D.; Ji, H.; Yang, Z. Functional characterization of three novel genes encoding Diacylglycerol Acyltransferase (DGAT) from oil–rich tubers of *Cyperus esculentus*. *Plant Cell Physiol.* **2020**, *61*, 118–129. [CrossRef]
73. Kaup, M.T.; Froese, C.D.; Thompson, J.E. A role for diacylglycerol acyltransferase during leaf senescence. *Plant Physiol.* **2002**, *129*, 1616–1626. [CrossRef]
74. Lu, C.L.; de Noyer, S.B.; Hobbs, D.H.; Kang, J.; Wen, Y.; Krachtus, D.; Hills, M.J. Expression pattern of diacylglycerol acyltransferase–1, an enzyme involved in triacylglycerol biosynthesis, in *Arabidopsis thaliana*. *Plant Mol. Biol.* **2003**, *52*, 31–41. [CrossRef]

75. Zhang, C.; Zhang, Z.; Yang, J.B.; Meng, W.Q.; Zeng, L.L.; Sun, L. Genome–wide identification and relative expression analysis of DGATs gene family in sunflower. *Acta Agron. Sin.* **2023**, *49*, 73–85.
76. Zhao, Y.P.; Wu, N.; Li, W.J.; Shen, J.L.; Chen, C.; Li, F.G.; Hou, Y.X. Evolution and Characterization of Acetyl Coenzyme A: Diacylglycerol Acyltransferase Genes in Cotton Identify the Roles of GhDGAT3D in Oil Biosynthesis and Fatty Acid Composition. *Genes* **2021**, *12*, 1045. [CrossRef] [PubMed]
77. Takeda, S.; Iwasaki, A.; Matsumoto, N.; Uemura, T.; Tatematsu, K.; Okada, K. Physical interaction of floral organs controls petal morphogenesis in *Arabidopsis*. *Plant Physiol.* **2013**, *161*, 1242–1250. [CrossRef] [PubMed]